

ECCD studies for EU-DEMO plasmas

Emanuele Poli^{1,*}, Lorenzo Figini², Emiliano Fable¹, Mattia Siccino^{1,3}, Antti Snicker⁴, Chuanren Wu⁵, and Hartmut Zohm¹

¹Max-Planck-Institut für Plasmaphysik, 856748 Garching bei München, Germany

²Istituto di Scienza e Tecnologia dei Plasmi, CNR, 20125 Milano, Italy

³EUROfusion-Consortium, 85748 Garching bei München, Germany

⁴VTT, 02044 Espoo, Finland

⁵Karlsruhe Institute of Technology (KIT), 76344 Eggenstein-Leopoldshafen, Germany

Abstract. The possibility of driving a large fraction of the plasma current in a tokamak reactor employing electron cyclotron waves is investigated for scenarios as envisaged in the European DEMO through beam tracing calculations performed with the TORBEAM code, which assumes a linear regime for power absorption and employs an adjoint method for the determination of the driven current. Comparatively high ECCD efficiency in the inner half of the plasma column can be achieved by injecting the wave from an elevated position. On the other hand, the efficiency deteriorates in the colder, outer part of the plasma, so that a prohibitive amount of power would be needed to sustain the plasma current non-inductively by ECCD only in the considered scenarios. As an alternative scheme, the injection of slow extraordinary wave below the fundamental resonance is considered. The basic physics features of this scenario are discussed.

1 Introduction

The European plans for a demonstration fusion reactor aim at the realization of a tokamak that has the among its main goals the production of net electricity (ca. 500 MW, corresponding to a fusion power of ca. 2 GW), the evidence for reliable solutions to the problem of tritium self-sufficiency and the adoption of maintenance systems that can ensure adequate plant availability [1]. A typical set of plasma and machine parameters can be found e.g. in Table 1 of [2]. Although the final design point has not been fixed yet and several options have been explored, a common feature of the EU-DEMO is to represent a "modest extrapolation from the ITER physics and technology basis." [3].

In a power-plant environment, a heating and current drive system based on the injection of electron cyclotron (EC) waves is particularly attractive, as it presents no intrinsic coupling issues (EC waves propagate in vacuum) and the launchers/antennas do not need to be located close the plasma. Moreover, the injection of the wave requires only small openings in the blanket. Finally, EC waves offer the possibility of localized plasma control. The present target design for DEMO is a pulsed machine (duration of the plasma discharge ca. 2 hours [1]) and the main functions under consideration for the EC system are assisted breakdown, start up and current ramp control; control of magnetohydrodynamic instabilities; bulk heating of the core plasma; control of the radiative instability caused by abrupt impurity penetration in the outer plasma [4]. In this context, steady state operation is not envisaged and

electron cyclotron current drive (ECCD) are not supposed to sustain a significant part of the plasma current. In the first part of this paper, the injected power that would be needed to achieve nearly steady-state conditions is estimated for a specific set of DEMO parameters. The current drive efficiency is found to drop in the outer half of the plasma column, mainly because of the unfavourable scaling with the ratio T_e/n_e [5] (here T_e is the electron temperature and n_e the electron density). The very large power that would be necessary to sustain the plasma current profile non-inductively makes this scheme unattractive and is one of the reasons for considering a pulsed tokamak as the baseline choice. An alternative which has been considered recently in the frame of the ECCD studies for the STEP tokamak is injection of first-harmonic extraordinary mode (X1) [6]. In this scheme, the cutoff which is usually encountered in X1 schemes for injection from the low-field side (LFS) is avoided by selecting a wave frequency which is low enough to place the cold resonance outside the plasma. A first investigation of the physics behind this ECCD scenario and its possible advantages is presented in the second part of this paper.

2 Synthesizing a broad current profile with ECCD

A DEMO scenario simulated with the transport code AS-TRA [7] is considered, in which approximately 48% of the plasma current is generated through external heating. The main plasma parameters are a magnetic field on axis $B_0 = 5.8$ T, major radius $R_0 = 8.4$ m, minor radius

*e-mail: emanuele.poli@ipp.mpg.de

Table 1. Power assigned to each profile shown in Fig. 3 to obtain the synthetic profiles reported in Fig. 4.

prof1	prof2	prof3	prof4	prof5	prof6	prof7	prof8	prof9	prof10	
1 MW	7 MW	4 MW	7 MW	15 MW	15 MW	0 MW	0 MW	70 MW	40 MW	Total 159 MW
0 MW	10 MW	5 MW	45 MW	70 MW	40 MW	Total 170 MW				

$a = 2.88$ m, effective charge $Z_{\text{eff}} = 1.48$, central density $n_{e0} = 8 \times 10^{19} \text{ m}^{-3}$ and central electron temperature $T_{e0} = 35$ keV, see Fig. 1.

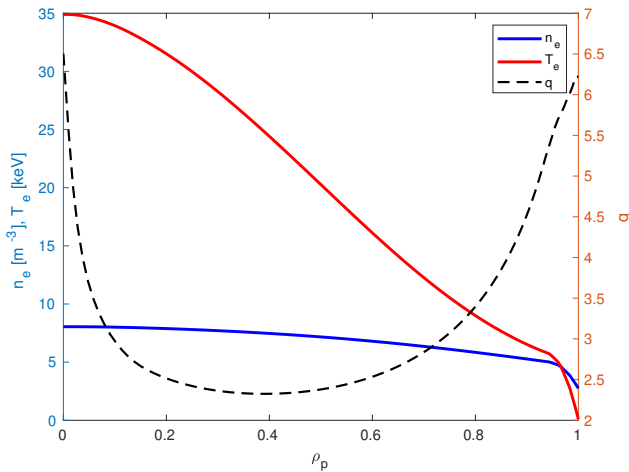


Figure 1. Electron density (blue), electron temperature (red) and safety factor (black dashed) as a function of the normalized poloidal radius ρ_p for the DEMO scenario under consideration.

In the ASTRA simulation, an off-axis current drive profile is assumed, scaled in such a way that the global current drive efficiency is 50 kA/MW. The fact that the driven-current profile is peaked off axis and contains most of the current in the region $0.3 < \rho_p < 0.9$ (Fig. 2) implies that a large current drive is needed in this scenario in regions where the plasma temperature is around 10 keV, i.e. significantly lower than at the centre.

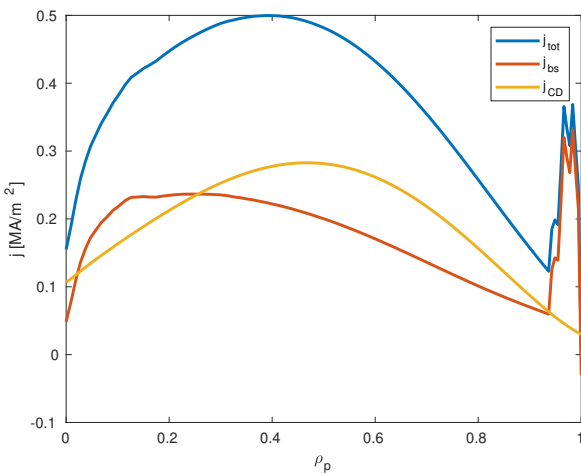


Figure 2. Radial profiles of the total current density (blue), bootstrap current density (red) and externally-driven current density (yellow).

While the current drive efficiency of 50 kA/MW assumed in ASTRA can be considered as realistic for ECCD in the centre of the plasma [8], EC waves cannot achieve

this efficiency in the outer part of the plasma column (while it could be probably achieved with Neutral Beam Injection [9]). In order to "synthesize" through ECCD a profile similar to that assumed in ASTRA, the achievable driven current has been evaluated with the TORBEAM code [10] for different launch positions, launch angles and frequencies, assuming absorption at the fundamental harmonic with ordinary-mode (O1) polarization. In particular, it is known both theoretically [8, 11] and experimentally [12] that injection from an elevated position can lead to an enhanced current drive efficiency (the maximum current drive conditions for top launch are usually achieved at slightly higher frequencies than in the case of midplane launch).

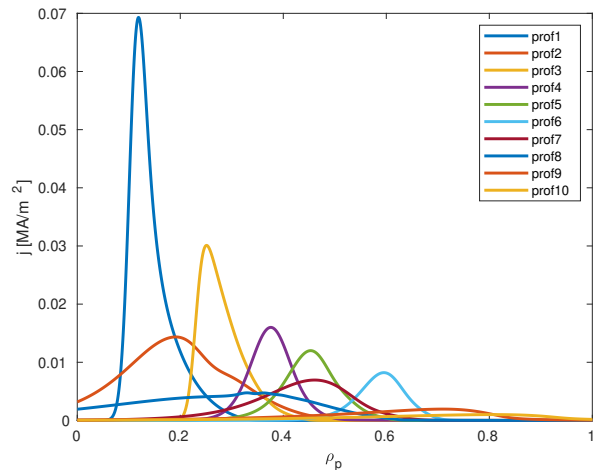


Figure 3. ECCD profiles used to synthesize the profile of the driven current as shown in Fig. 4.

A collection of "optimum" ECCD profiles peaked at different positions is shown in Fig. 3. They are obtained employing launch points with an elevation Z above the midplane between 4 and 5.5 m and frequencies between 220 and 240 GHz. The injected power is 1 MW. The decrease of the peak current density with radius is due to both the decreasing T_e/n_e and the increasing surface on which the current is distributed.

Fig. 4 shows two different combinations of the profiles displayed in Fig. 3, one obtained with a total injected power of 159 MW (blue curve), and one with 170 MW (red curve). The power injected for each profile is reported in Table 1. Despite the large injected power, both curves are actually still below the reference ASTRA profile (yellow). It is in particular important to note that 110 MW flow into the two most external profiles. It is clear that an injected power of the order of 200 MW is unattractive in terms of balance of plant, because even in the optimistic case of an efficiency of the EC system of the order of 50%, the total required power is comparable to the net electrical output of the reactor. It should be remarked that the high

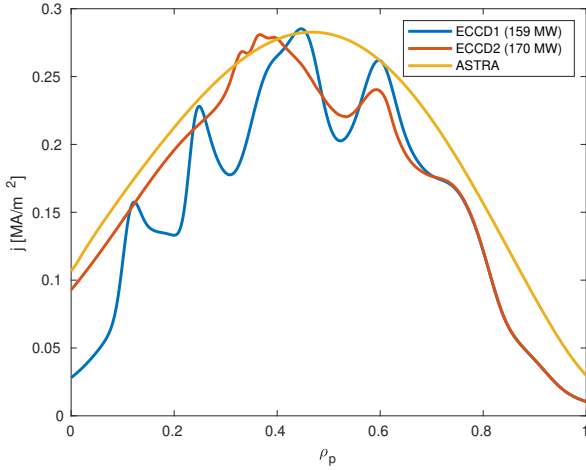


Figure 4. The yellow curve represents the target externally-driven current density profile used in the ASTRA simulations of the DEMO scenario under consideration. The blue and the red curve show two different possibilities of combining the profiles displayed in Fig. 3 (employing 159 resp. 170 MW) to reproduce the target current-drive profile.

temperature and the comparatively low density of this scenario represent quite favourable conditions for ECCD. On the other hand, optimizing a (nearly) steady-state scenario with particular attention to the best conditions for high ECCD efficiency might lead to less severe requirements in terms of injected power.

3 Electron cyclotron current drive employing extraordinary mode at the fundamental harmonic

Extraordinary mode at the fundamental harmonic is usually not considered as a viable heating scheme in magnetic-confinement fusion, due to the fact that the cyclotron resonance is screened by a cutoff layer for LFS injection. Moreover, the absorption drops to zero for propagation perpendicular to the equilibrium magnetic field. A way to avoid the cutoff for LFS launch is to choose a sufficiently low wave frequency that the cutoff moves outside the plasma. In this case, also the cold resonance moves close to or outside the edge of the plasma. However, for ECCD schemes (where a finite parallel wavevector is required), one can rely on the Doppler shift to move the absorption region inside the (outer part of) the plasma. Preliminary results suggest that this might lead to a high ECCD efficiency in spherical tokamaks [6]. In this section, the physics behind this scheme is discussed in the frame of the model implemented in codes that use an adjoint scheme [13] for the determination of the ECCD efficiency. Following the notation of Lin-Liu *et al.* [14], the current density driven by the EC waves can be written in terms of the response function χ as

$$j_{||} \propto mu_e^2 \int d\gamma u_{\perp}^2 f_M \tilde{\Lambda} \chi, \quad (1)$$

where m is the electron mass, $u_e = \sqrt{2T_e/m}$ is the electron thermal velocity, f_M is the (Maxwellian) equilibrium distribution function and ([14], Eq. 39)

$$mu_e^2 \tilde{\Lambda} \chi = \text{sgn}(u_{||}) \frac{\gamma u_e^2}{u} \left\{ \frac{dF}{du} H + 2 \frac{B_{\max}}{B} \frac{u_{||}}{u^2} \left(\frac{u_{||}}{u} - \frac{N_{||} u}{\gamma c} \right) F \frac{dH}{d\lambda} \right\} \quad (2)$$

(B_{\max} is the maximum value of the magnetic field on a given flux surface). The previous expression is based on the fact that the response function can be factorized in a part depending on the absolute value of the momentum and a part depending on the pitch angle $\lambda = B_{\max} u_{\perp}^2 / Bu^2$ as $\chi = \text{sgn}(u_{||}) F(u) H(\lambda)$. In Eq.(1), the integral is performed with respect to the Lorentz factor $\gamma = \sqrt{1 + u_{\perp}^2 + u_{||}^2}$, where the components of the relativistic momentum per unit mass $\mathbf{u} = \gamma \mathbf{v}$ are expressed as a function of γ making use of the resonance condition. Before proceeding, it is observed that the ECCD model contained in the TORBEAM code and used to produce the plots below contains a slightly more advanced model than that discussed in [14], e.g. the response function includes a correction for momentum conservation as in [15]. However, the basic physical picture remains the same.

In order to get a grasp of the physics described by the previous equations, it is useful to consider first as an example the case of bulk current drive near the plasma centre with fundamental-harmonic ordinary mode (O1), which is the standard scheme for ECCD in ITER and DEMO, cf. also Sec. 2 above. In this case, the response function χ and the resonance condition at the position of maximum absorption exhibit the typical velocity-space structure that can be seen in Fig. 5. The plasma parameters considered here correspond to a “low-aspect-ratio” DEMO, with reduced major radius (as compared to Sec. 2) $R_0 = 7.5$ m and magnetic field $B_0 = 4$ T.

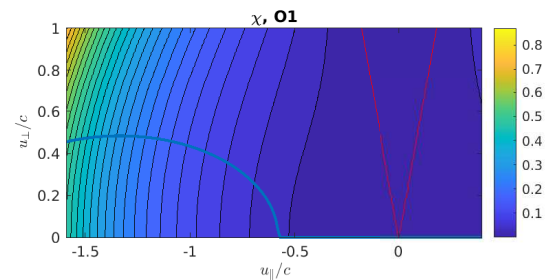


Figure 5. Response function χ in velocity space (coloured levels) for a typical O1 scenario with absorption close to the plasma centre. The blue ellipse represents the resonance condition, the red lines show the trapping cone.

The contour levels of the response function χ show an increase with u (a scaling $F \propto u^4$ is expected in the non-relativistic limit [16]). The trapping cone is narrow because the EC power is deposited close to the axis in this case. Moreover, the conditions for optimum Fisch-Boozer current drive [17] require the resonance to be on

high-energy passing electrons, as long as this is compatible with sufficiently high absorption, cf. [11] and references therein. The strongest wave-particle interaction in velocity space occurs on the part of the resonance curve that is closest to the Maxwellian bulk, where most of the electrons reside (apart from the region very close to the u_{\parallel} -axis, as a finite u_{\perp} is required for the cyclotron interaction to take place). In this region, the resonance curve intersects the contours levels of χ almost along the lines of steepest F -increase, while the change of H (function of u_{\perp}/u) is small. Correspondingly, the main contribution of $\tilde{\Lambda}\chi$ to the integral in Eq.(1) stems from the first term inside brackets on the right-hand side of Eq.(2).

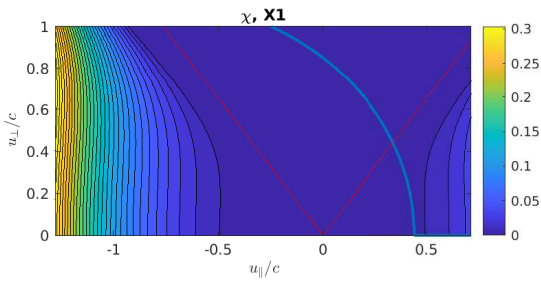


Figure 6. Response function χ in velocity space (coloured levels) for a typical X1 scenario with absorption close to the plasma edge. The blue ellipse represents the resonance condition, the red lines show the trapping cone.

The situation described above differs substantially from the X1 ECCD scenario considered here, where the power is absorbed in the outer part of the plasma. (Fig. 6). First of all, the trapping cone is much wider and its impact on the contour levels of the response function χ is much more evident than in Fig. 5. In particular, the function $H(\lambda)$ in χ drops rapidly to zero approaching the passing/trapped boundary. Second, since the resonant wave-particle interaction takes place on the high-field side of the cold resonance, the resonance curve is not confined to the region of negative velocities, like in the O1 case. On the contrary, low-energy resonant electrons possess in this case a positive parallel velocity. Finally, and related to the previous point, in this X1 scheme the resonance curve intersects the trapping cone, while in the O1 scheme it is far from it. On the basis of these observations, it might be expected that for the X1 scheme the term proportional to $FdH/d\lambda$, i.e. the second term in the brackets on the right-hand side of Eq.(2), dominates the ECCD efficiency.

Fig. 7 shows a comparison of the various terms in Eq. (1) for the O1 scheme. The red dashed line reproduces the product $u_{\perp}^2 f_M \equiv \alpha$, which is zero where the resonance curve intersects the u_{\parallel} -axis (i.e. where $u_{\perp} = 0$) and is peaked at the low-energy end on the resonance curve, $-0.7 \lesssim u_{\parallel}/c \lesssim -0.6$, because of the Maxwellian factor. The yellow solid line represents the first term on the right-hand side of Eq.(2), proportional to HdF/du , which increases for larger values of u_{\parallel} . This term clearly dominates over the second term on the right-hand side of the same equation, shown by the solid purple line. Overall,

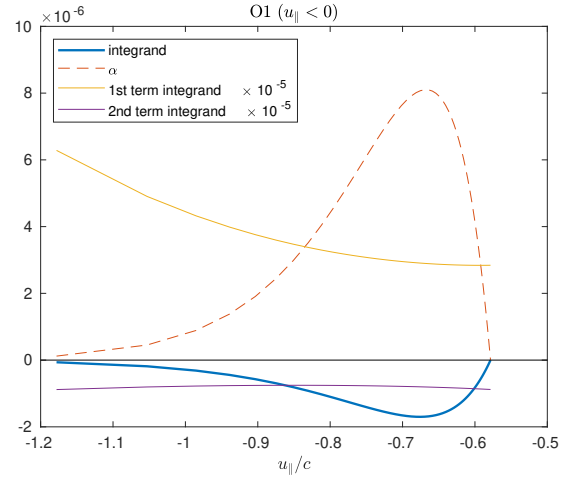


Figure 7. Contribution of different terms to the integrand of Eq.(1) for O-mode ECCD close to the plasma centre as a function of u_{\parallel} .

the integrand in Eq.(1) is negative because the sign of u_{\parallel} is minus along the whole resonance curve. The peak of the integrand (solid blue line) reflects the peak of the α factor.

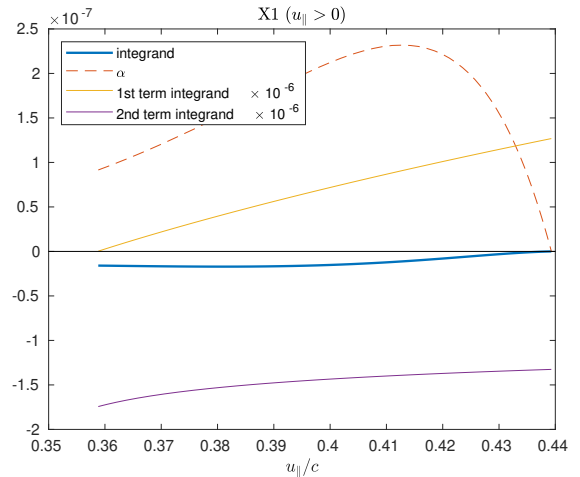


Figure 8. Contribution of different terms to the integrand of Eq. (1) for X-mode ECCD close to the plasma edge as a function of u_{\parallel} .

Again, the situation is very different for the X1 scheme (Fig. 8). The electrons contributing to ECCD lie on the part of the region where $u_{\parallel} > 0$. The contribution of the region with $u_{\parallel} < 0$ is very small because the resonance can be satisfied there only by very energetic electrons, whose number is extremely small. Since the response function is set to zero inside the trapping cone [14], the relevant range is between the intersection of the resonance curve with the trapping cone and that with the u_{\parallel} -axis, see Fig. 6. Note that while u_{\perp} is zero at the latter point, it is not at the former. It can be seen from Fig. 8 that, as discussed above, the second term on the right-hand side of Eq.(2), represented by the purple line, is now larger (in absolute value) than the first one. Since this term is neg-

ative¹, one might expect that the current is now driven in the opposite direction as compared to the O1 scheme discussed before. The electrons contributing to ECCD, however, have now a positive parallel velocity, so that the term $\text{sgn}(u_{\parallel})$ is also opposite as compared to the O1 case. As a consequence, in both schemes the current is driven in the same direction if the EC beams are injected in the same toroidal direction.

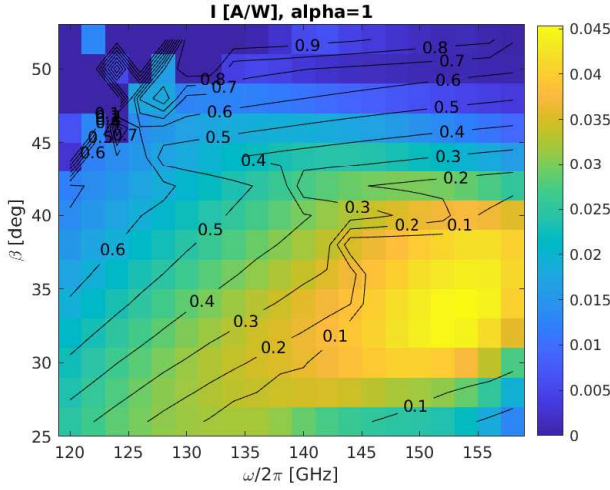


Figure 9. Total driven current (colour) per injected MW as a function of the beam frequency $\omega/2\pi$ and of the toroidal launch angle β . The wave is injected with O-mode polarization. The black contours represent ρ_p at the position of maximum absorption.

Fig. 9 and 10 show the total driven current as a function of the wave frequency $\omega/2\pi$ and of the toroidal injection angle (injection from the midplane is considered for simplicity), and the poloidal launch angle is zero. In the plots, the black lines denote the radial position of the peak current density for each value of frequency and toroidal launch angle. It can be seen that for the O1 scenario, the maximum current drive is obtained close to the centre employing frequencies above 150 GHz, and is just above $I_{CD} = 45$ kA/MW. The ECCD drops rapidly when the deposition occurs in the outer part of the plasma and close to the edge. This is similar to the situation discussed in Sec. 2.

For X1 injection, on the other hand, the maximum ECCD is found in the outer part of the plasma and is around 15 kA/MW in a relatively broad range between $0.6 < \rho_p < 0.9$, employing frequencies in the range of 65 GHz. While these values are still significantly below the current drive efficiency of 50 kA/MW that was assumed in the ASTRA simulations mentioned in Sec. 2, they represent an improvement with respect to the O1 results. An analysis of the normalized efficiency $\zeta_{CD} \propto (n_e/T_e)(I_{CD}/P)$ (Fig. 11) also reveals that X1 injection has a normalized efficiency comparable or even higher than for the case of O1 (which peaks around 0.4 for central deposition, not shown here).

¹The fact that the term proportional to $FdH/d\lambda$ (purple line) is negative as in the O1 case is due to a sign reversal of both u_{\parallel} and the term $u_{\parallel}/u_{\perp} - N_{\parallel}u_{\parallel}/\gamma c$ within parenthesis in Eq.(2).

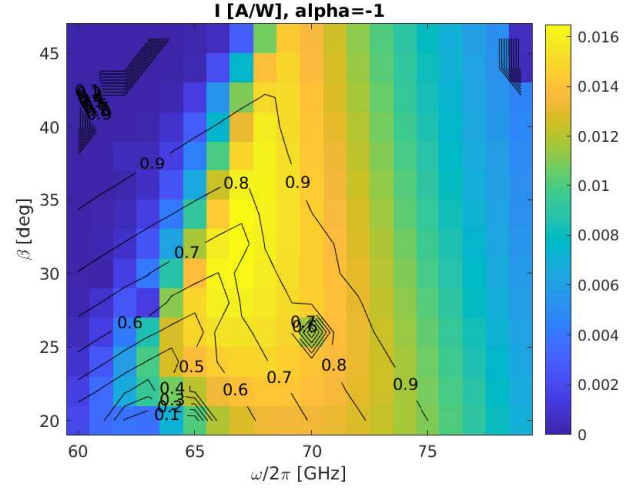


Figure 10. Same as Fig. 9 but for X-mode injection.

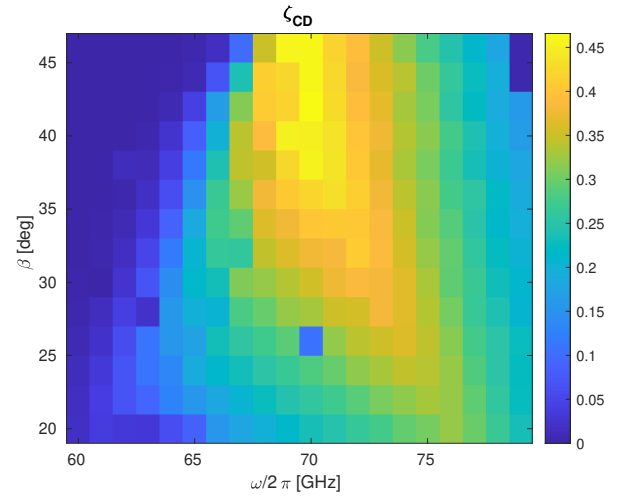


Figure 11. Normalized efficiency $\zeta_{CD} \propto (n_e/T_e)(I_{CD}/P)$ for X-mode injection.

The normalized efficiency ζ_{CD} can be considered as a measure of the “phase space efficiency” of ECCD, since it takes into account already its basic T_e/n_e scaling [18]. In particular, ζ_{CD} is found to increase with ρ_p , which can be ascribed to the increase of the trapped particle fraction with radius. This might also explain the high efficiency for spherical-tokamak geometry [6].

Some words of caution are appropriate at the end of this section. From the analysis presented above, it is clear that the main contribution to the driven current in the X1-scenario comes from the fast drop of the response function when the passing/trapped boundary is approached, see Fig. 6 and 8. This physics is closely reminiscent of the Ohkawa effect [19]. In the case under consideration, where the resonant interaction takes place on the LFS of the cold resonance, the resonance curve runs from $u_{\perp} = 0$ towards the trapping cone, intersecting its boundary almost perpendicularly in the $(u_{\parallel}, u_{\perp})$ -plane. This represents a difference with respect to the standard analysis of the Ohkawa current drive, where the resonance curve is usually considered to approach the passing/trapped boundary

tangentially, cf. e.g. Fig.10 of [20]. The treatment of the relevant physics adopted in TORBEAM, based on the adjoint model, might lack the desired accuracy in describing the details of the electron response in this region of velocity space. A solution of the full Fokker-Planck equation [21] would be desirable to assess the quantitative validity of the predictions presented here.

4 Conclusions

In this paper, it has been shown that replacing a large fraction of the plasma current through ECCD, as would be required for steady state scenarios, typically requires an injected power which is not compatible with an advantageous balance of plant in a fusion reactor. The main problem is related to the drop of ECCD efficiency in the outer part of the plasma. The X1 scenario first discussed in [6] has been investigated in some detail on the basis of linear beam tracing calculation that employ an adjoint method for the calculation of the ECCD efficiency. Although some attractive features of this scheme emerged, and there is probably still some room for further optimization, the increase in ECCD efficiency might be still too low from the point of view of steady-state operation. Also the accuracy of the modelling should be compared to more physically comprehensive Fokker-Planck simulations.

Quasilinear calculations could be performed to check the validity of the linear modelling employed here as well. According to [22], a deviation from a linear behaviour should be observed when the power density exceeds a threshold of the order of $0.5 \times n_{19}^2$ MW/m³, where n_{19} is the electron density in units of 10^{19} m⁻³. For typical DEMO parameters, this corresponds to a power density of ca. 50 MW/m³, which can be reached only very close to the magnetic axis of the plasma, even if the injected power exceeds 100 MW.

Finally, it should be mentioned that the X1 scheme discussed here, although theoretically appealing, would likely imply that the cold resonance would be located close to or inside the launcher. This might have severe consequences for the integrity of the launcher components. This is an aspect that should be kept in mind if further studies will confirm the attractiveness of this scenario in terms of ECCD efficiency.

Acknowledgement This work has been carried out within the framework of the EUROfusion Consortium, funded by the European Union via the Euratom Research and Training Programme (Grant Agreement No 101052200 — EUROfusion). Views and opinions expressed are however those of the author(s) only and do not necessarily reflect those of the European Union or the European Commission. Neither the European Union nor the European Commission can be held responsible for them.

References

[1] G. Federici *et al.*, *DEMO design activity in Europe: Progress and updates*, Fus. Eng.Des. **136**, 729 (2018).

- [2] R. Kembleton *et al.*, *EU-DEMO design space exploration and design drivers*, Fus. Eng.Des. **178**, 113080 (2022).
- [3] G. Federici *et al.*, *The EU DEMO staged design approach in the Pre-Concept Design Phase*, Fus. Eng.Des. **173**, 112959 (2021).
- [4] T. Franke *et al.*, *Integration concept of an electron cyclotron system in DEMO*, Fus. Eng.Des. **168**, 112653 (2021).
- [5] M. Brambilla, *Kinetic Theory of Plasma Waves* (Oxford University Press, 1998).
- [6] L. Figini *et al.*, 21st EC Workshop, Contribution #91 (ITER Organization, June 20-24 2022), unpublished.
- [7] G. V. Pereverzev, P. N. Yushmanov, *ASTRA: Automated System for Transport Analysis in Tokamaks*, IPP Report 5/98 (2002).
- [8] E. Poli *et al.*, *Electron-cyclotron-current-drive efficiency in DEMO plasmas*, Nucl. Fusion **53**, 013011 (2013).
- [9] F. Wagner *et al.*, *On the heating mix of ITER*, Plasma Phys. Control. Fusion **52**, 124044 (2010).
- [10] E. Poli *et al.*, *TORBEAM 2.0, a paraxial beam tracing code for electron-cyclotron beams in fusion plasmas for extended physics applications*, Comp. Phys. Comm. **225**, 36 (2018).
- [11] E. Poli *et al.*, *Fast evaluation of the current driven by electron cyclotron waves for reactor studies*, Phys. Plasmas **25**, 125001 (2018).
- [12] Xi Chen *et al.*, *Doubling off-axis electron cyclotron current drive efficiency via velocity space engineering*, Nucl. Fusion **62**, 054001 (2022).
- [13] T. M. Antonsen and K. R. Chu, *Radio frequency current generation by waves in toroidal geometry*, Phys. Fluid **25**, 1295 (1982).
- [14] Y. R. Lin-Liu *et al.*, *Electron cyclotron current drive efficiency in general tokamak geometry*, Phys. Plasmas **10**, 4064 (2003).
- [15] N. B. Marushchenko *et al.*, *Electron cyclotron current drive calculated for ITER conditions using different models*, Nucl. Fusion **48**, 054002 (2008).
- [16] M. Taguchi, *ECRH current drive in tokamak plasmas*, Plasma Phys. Control. Fusion **31**, 241 (1989).
- [17] N. J. Fisch and A. H. Boozer, *Creating an asymmetric plasma resistivity with waves*, Phys. Rev. Lett. **45**, 720 (1980).
- [18] T. C. Luce *et al.*, *Generation of localized noninductive current by electron cyclotron waves on the DIII-D tokamak*, Phys. Rev. Lett. **83**, 4550 (1999).
- [19] T. Ohkawa, *Steady state operation of tokamaks by rf heating*, General Atomics Report **GA-A13847** (1976).
- [20] R. Prater, *Heating and current drive by electron cyclotron waves*, Phys. Plasmas **11**, 2349 (2004).
- [21] C. F. F. Karney, *Fokker-Planck and quasilinear codes*, Comp. Phys. Rep. **4**, 183 (1986).
- [22] R. W. Harvey *et al.*, *Power dependence of electron-cyclotron current drive for low- and high-field absorption in tokamaks*, Phys. Rev. Lett. **62**, 426 (1989).